

# Experimental realization of a Weyl semimetal phase with Fermi arc surface states in TaAs

Su-Yang Xu\*,<sup>1</sup> Ilya Belopolski\*,<sup>1</sup> Nasser Alidoust\*,<sup>1</sup> Madhab Neupane\*,<sup>1,2</sup> Chenglong Zhang,<sup>3</sup> Raman Sankar,<sup>4</sup> Shin-Ming Huang,<sup>5,6</sup> Chi-Cheng Lee,<sup>5,6</sup> Guoqing Chang,<sup>5,6</sup> BaoKai Wang,<sup>5,6,7</sup> Guang Bian,<sup>1</sup> Hao Zheng,<sup>1</sup> Daniel S. Sancez,<sup>1</sup> Arun Bansil,<sup>7</sup> Fangcheng Chou,<sup>4</sup> Hsin Lin,<sup>5,6</sup> Shuang Jia,<sup>3</sup> and M. Zahid Hasan<sup>1</sup>

<sup>1</sup>*Joseph Henry Laboratory, Department of Physics,  
Princeton University, Princeton, New Jersey 08544, USA*

<sup>2</sup>*Condensed Matter and Magnet Science Group,  
Los Alamos National Laboratory, Los Alamos, NM 87545, USA*

<sup>3</sup>*ICQM, School of Physics, Peking University*

<sup>4</sup>*Center for Condensed Matter Sciences,  
National Taiwan University, Taipei 10617, Taiwan*

<sup>5</sup>*Centre for Advanced 2D Materials and Graphene  
Research Centre National University of Singapore,*

*6 Science Drive 2, Singapore 117546*

<sup>6</sup>*Department of Physics, National University of Singapore,*

*2 Science Drive 3, Singapore 117542*

<sup>7</sup>*Department of Physics, Northeastern University,*

*Boston, Massachusetts 02115, USA*

(Dated: May 30, 2022)

---

\* These authors contributed equally to this work.

## Abstract

A Weyl semimetal is a gapless topological state of matter described by a unique bulk-boundary correspondence in the electronic band structure. The low-energy bulk electrons are linearly-dispersing Weyl fermions, while the Weyl nodes are connected on the boundary by Fermi arc surface states. Using angle-resolved photoemission spectroscopy, we show that the inversion-breaking single crystalline compound TaAs hosts an electronic structure with Fermi arc surface states. We directly observe that these Fermi arc surface states terminate into the bulk bands and that these bulk bands disperse linearly, forming Weyl cones. These results are remarkably consistent with recent theoretical predictions of a Weyl semimetal phase in this compound. Our detailed surface and bulk band structure measurements demonstrate that TaAs hosts topologically non-trivial Fermi arcs and Weyl cones, providing the first experimental realization of a Weyl semimetal in condensed matter physics.

The rich correspondence between high energy and condensed matter physics has led to a deeper understanding of spontaneous symmetry breaking, phase transitions, renormalization and many other fundamental phenomena in nature, with important consequences for practical applications using magnets, superconductors and other novel materials [1–7]. Recently, there has been considerable progress in realizing particles previously considered in high energy physics as emergent quasiparticle excitations of crystalline solids, such as Dirac or Majorana fermions [8–15].

The recent discoveries of Dirac fermions in graphene and on the surface of topological insulators have ignited worldwide interest in physics and materials science [9–11]. Materials that host these exotic particles exhibit unique properties and hold promise for applications such as fault-tolerant quantum computation, low-power electronics and spintronics. A Weyl semimetal is an unusual crystal where the bulk electrons also behave as massless quasiparticles with linear dispersions but interestingly they differ from Dirac fermions seen in graphene or topological insulators in profoundly topological way. The Weyl fermions were originally considered in particle physics in connection to neutrinos but neutrinos were later found to have a small mass. A topological Weyl semimetal provides a condensed matter realization of Weyl fermions in the crystals bulk but possesses bulk-boundary correspondence in the sense that they must have very unusual forms of surface states. The signature of the topology of a Weyl semimetal in real materials is the existence of unusual Fermi arc surface states, which can be viewed as half of a surface Dirac cone in a topological insulator realized in a gapless material. Both the Weyl fermions in the bulk and the Fermi arc states on the surface of a Weyl semimetal are predicted to show unusual transport phenomena, which can be potentially used in future device applications. Weyl fermions in the bulk can give rise to negative magnetoresistance, the quantum anomalous Hall effect, non-local transport and local non-conservation of ordinary current [16–19]. Fermi arc states on the surface are predicted to show novel quantum oscillations in magneto-transport and quantum interference effects in tunneling spectroscopy [20–22]. Because of the fundamental and practical interest in Weyl semimetals, it is crucial that robust candidate materials be found.

Despite interest, a Weyl semimetal remains elusive in real materials. Here, in this paper, we present the first experimental realization of a Weyl semimetal in Tantalum arsenide (TaAs) single crystals. This material has recently been predicted as a robust Weyl semimetal candidate [23, 24]. We also for the first time demonstrate the nontrivial topological nature

of the gapless semimetal state in TaAs. Using angle-resolved photoemission spectroscopy, we show that the inversion-breaking single crystalline compound TaAs hosts an electronic structure with Fermi arc surface states. We directly observe that these Fermi arc surface states terminate into the bulk bands and that these bulk bands disperse linearly, forming Weyl cones. These results are remarkably consistent with recent theoretical predictions of a Weyl semimetal phase in this compound. Our discovery of the Weyl semimetal phase opens an entirely new era in condensed matter and materials physics.

Tantalum arsenide, TaAs, crystallizes in a body-centered tetragonal lattice system (Fig. 1a) [25]. The lattice constants are  $a = 3.437 \text{ \AA}$  and  $c = 11.646 \text{ \AA}$ , and the space group is  $I4_1md$  (#109,  $C_{4v}$ ). The crystal consists of interpenetrating Ta and As sub-lattices, where the two sub-lattices are shifted by  $(\frac{a}{2}, \frac{a}{2}, \delta)$ ,  $\delta \approx \frac{c}{12}$ . There are two Ta atoms and two As atoms in each primitive unit cell. In order to verify the crystal structure, we perform X-ray diffraction measurements of the TaAs single crystals used in our study, shown in Fig. 1c. Our diffraction data matches well with the lattice parameters and the space group of  $I4_1md$ . Thus our XRD measurements demonstrate the lack of inversion symmetry in our TaAs single crystal. This is important because otherwise a Weyl semimetal phase is not possible. To further check the chemical composition of our samples, we also present an ARPES core level spectrum measured in Fig. 1b. Clear Ta  $4f$  and As  $3d$  core level peaks are observed. Furthermore the intensity ratio between the Ta  $4f$  and As  $3d$  peaks is close to 1 : 1. These measurements further confirm the chemical composition of our TaAs samples.

Fig. 1e shows a brief overview of our ARPES results and an overview of our numerical calculation of the TaAs band structure is presented in 1f. We observe Fermi arcs near the  $\bar{X}$  point, and near the midpoint of the  $\bar{X}$  point and the  $\bar{\Gamma}$  point (similarly, arcs are observed near the  $\bar{Y}$  point, as well as the midpoint of the  $\bar{Y}$  point and the  $\bar{\Gamma}$  point). We find a good agreement between these Fermi arcs observed in our ARPES measurements and those predicted from our theoretical model, providing conclusive evidence that we have discovered the first Weyl semimetal.

We also note that the  $C_4$  rotational symmetry is broken at the (001) surface because the system is only invariant under a four-fold rotation with a translation along the out-of-plane direction. The bulk and (001) surface Brillouin zones (BZ) are shown in Fig. 1b, where high symmetry points are also noted.

We next present ARPES spectra on TaAs showing the Fermi arc surface states which

are a key signature of a Weyl semimetal. We observe a square Brillouin zone, suggesting that we are measuring on the (001) surface of the bulk crystal (see Fig. 2a). At deeper binding energies, we further note that the bands are  $C_4$  symmetric, which is consistent with the  $C_4$  rotation symmetry axis of TaAs and confirms that we are studying the (001) cleaving plane, perpendicular to this rotation axis. We can summarize the constant-energy contours of the band structure at deeper binding energies as a set of tiled circles, with a large circle concentric with the  $\bar{\Gamma}$  point and a smaller circle consistent with the  $\bar{M}$  point (surface Brillouin zone corner). The regions in between the tiled circles surround the  $\bar{X}$  and  $\bar{Y}$  points. These experimental measurements of the bulk band structure of TaAs at deeper binding energies are also in agreement with *ab initio* band structure calculations. We next consider the band structure at shallow binding energies. We observe that  $C_4$  symmetry is strongly violated at and near the Fermi level. This is entirely consistent with the bulk crystal structure of TaAs, where the rotational symmetry is implemented as a screw axis which sends the crystal back into itself only after a  $C_4$  rotation and a translation by  $c/2$  along the rotation axis. As a result, the (001) surface in fact breaks the rotational symmetry of the crystal. Our observed Fermi surface and its symmetries provide clear evidence that the bands we observe at shallow binding energies consist predominantly of surface states. We can summarize the band structure as consisting of surface state pockets enclosing the  $\bar{X}$  and  $\bar{Y}$  points with additional pockets located away from the high symmetry points (near the midpoint of the  $\bar{X}$  point and the  $\bar{\Gamma}$  point and near the midpoint of the  $\bar{Y}$  point and the  $\bar{\Gamma}$  point). In Fig. 2b we present a high-quality constant-energy contour of these surface states at the midpoint of the  $\bar{X}$  point and the  $\bar{\Gamma}$  point. We observe two crescents which touch together at their endpoints. Unlike topological surface states or trivial Rashba surface states, which form closed Fermi surfaces, these contours are open curves with endpoints, namely Fermi arcs. These Fermi arc surface states are in excellent agreement with calculations for the (001) surface. We further note that the termination points are neither located at the time-reversal invariant momenta, nor do they lie along a symmetry axis of the Brillouin zone. This suggests that at the endpoints of these Fermi arcs, the electron wavefunction unravels into the bulk states of a Weyl cone, also in agreement with the theoretical prediction. The fact that two arcs emerge from each Weyl cone suggests that the chiral charge of the Weyl points at the endpoints of these arcs is  $\pm 2$ . Our observation of two copropagating Fermi arcs threading from each of these two Weyl points is consistent with the theoretical prediction

that on the (001) surface of TaAs, pairs of Weyl points of the same chirality project onto the same point of the surface Brillouin zone. To better understand these Fermi arc surface states, we present a high-symmetry cut of the band structure along the  $\bar{\Gamma}$ - $\bar{X}$  direction in Fig. 2c. We observe Fermi arcs surface states at the  $\bar{X}$  point as well as near the midpoint of  $\bar{X}$  and  $\bar{\Gamma}$ . At each midpoint we see a pair of surface states rising from the bulk at deeper binding energies and then crossing the Fermi level, giving rise to the concentric crescents discussed in 2b. These Fermi arc surface states are in excellent agreement with *ab initio* band structure calculations. Our ARPES measurements provide clear and conclusive evidence of Fermi arc surface states on the (001) surface of TaAs.

We next consider the bulk band structure of TaAs in greater detail. In 3b we present an ARPES spectrum along a cut shifted away from a high-symmetry axis and passing through the endpoint of the Fermi arc surface states discussed in 2b above. In this spectrum we observe pairs of Fermi arc surface states rising to the Fermi level, as discussed above. In addition, nested below the Fermi arcs we also observe a faint signature of the bulk Weyl cones, with the bulk linear dispersion roughly parallel to the dispersions of the Fermi arc surface states. We find clear evidence of the bulk Weyl cone dispersions by considering a progression of parallel cuts. In 3b we see that the Dirac cone feature disperses as a function of in-plane momentum. We see that the Weyl cone rises to the Fermi level near the in-plane momentum where the Fermi arc surface states terminate, consistent with *ab initio* band structure calculations. This is entirely expected from the theory of Weyl semimetals, which claims that Fermi arc surface states must terminate at bulk Weyl nodes. We also observe the  $C_4$  rotated cousins of these Weyl cones, shown in 3d. Here, we also see that the Weyl cone disperses as a function of in-plane momentum and that the cone rises to the Fermi level to meet the Fermi arc surface states. These Weyl cones are in excellent agreement with *ab initio* band structure calculations and show that TaAs is a Weyl semimetal.

## DISCUSSION

Our ARPES spectra show that we have experimentally observed the first Weyl semimetal. Our results are consistent with the theory of Weyl semimetals and are in agreement with our *ab initio* band structure calculations. To place our discovery in the broader context of topological phases of matter, we provide some general comments on the nature of the phase

transition between a trivial insulator, a Weyl semimetal and a topological insulator. When a system with inversion symmetry undergoes a topological phase transition between a trivial insulator and a topological insulator, the band gap necessarily closes at a Kramers' point. If we imagine moving the system through the phase transition by tuning a parameter  $m$ , then there will be a critical point where the system is gapless. In a system which breaks inversion symmetry, there will instead be a finite range of  $m$  where the system remains gapless, giving rise to a Weyl semimetal phase. In this way, the Weyl semimetal phase can be viewed as an intermediate phase between a trivial insulator and a topological insulator, where the bulk band gap of a trivial insulator closes and Weyl points of opposite chiral charge nucleate from the bulk band touchings. As  $m$  is varied, the Weyl points thread surface states through the surface BZ and eventually annihilate each other, allowing the bulk band gap to reopen with a complete set of surface states, giving rise to a topological insulator. This understanding of a Weyl semimetal as an intermediate phase between a trivial insulator and a topological insulator offers some insight into the closed Fermi surfaces we find in TaAs around the  $\bar{M}$  point of the top surface and the  $\bar{X}'$  point of the bottom surface. We propose that these surface states reflect the topological invariant we would find if we annihilated the Weyl points to produce a bulk insulator. We consider the bottom surface, and annihilate the Weyl points in pairs in the obvious way to remove all surface states along  $\bar{\Gamma} - \bar{X}$ . Then, we can annihilate the remaining Weyl points to produce two concentric Fermi surfaces around the  $\bar{X}'$  point. Since this is an even number of surface states, we find that this way of annihilating the Weyl points gives rise to a trivial insulator. If, instead, we annihilate the remaining Weyl points to remove the Fermi arc connecting them, only the closed Fermi surface would be left around  $\bar{X}'$ , giving rise to a topological insulator. A similar analysis applies to the top surface. Our experimental discovery of a Weyl semimetal in TaAs opens the way for the study of these effects for fundamental interest and novel devices.

- 
- [1] H. Weyl, *Zeitschrift Physik* **56**, 330 (1929).
  - [2] L. Balents, *Physics* **4**, 36 (2011).
  - [3] A. M. Turner and A. Vishwanath, arXiv:1301.0330 (unpublished).
  - [4] F. Wilczek, *Phys. Today* **51**, 11 (1998).

- [5] G. E. Volovik, *The Universe in a Helium Droplet* (Clarendon Press, Oxford, 2003).
- [6] F. D. M. Haldane, arXiv:1401.0529 (unpublished).
- [7] S. Murakami, *New. J. Phys.* **9**, 356 (2007).
- [8] J. Alicea, *Rep. Prog. Phys.* **75**, 076501 (2012).
- [9] A. K. Geim and K. S. Novoselov. *Nature Mater.* **6**, 183 (2007).
- [10] M. Z. Hasan and C. L. Kane, *Rev. Mod. Phys.* **82**, 3045 (2010).
- [11] X. L. Qi and S. C. Zhang, *Rev. Mod. Phys.* **83**, 1057 (2011).
- [12] Z. Wang, *et al.*, *Phys. Rev. B* **85**, 195320 (2012).
- [13] Z. Wang, *et.al.*, *Phys. Rev. B* **88**, 125427 (2013).
- [14] M. Neupane *et al.*, *Nature Commun.* **5**, 3786 (2014).
- [15] S.Y. Xu *et al.*, *Science* **347**, 294 (2015).
- [16] A. A. Zyuzin and A. A. Burkov, *Phys. Rev. B* **86**, 115133 (2012).
- [17] C.-X. Liu, P. Ye, and X.-L. Qi, *Phys. Rev. B* **87**, 235306 (2013).
- [18] P. Hosur and X.-L. Qi, *Comptes Rendus Physique* **14**, 857 (2013).
- [19] S. A. Parameswaran *et al.*, *Phys. Rev. X* **4**, 031035 (2014).
- [20] P. Hosur, *Phys. Rev. B* **86**, 195102 (2012).
- [21] T. Ojanen, *Phys. Rev. B* **87**, 245112 (2013).
- [22] A. C. Potter, I. Kimchi and A. Vishwanath, *Nature Commun.* **5**, 5161 (2014).
- [23] Shin-Ming Huang\*, Su-Yang Xu\*, Ilya Belopolski\*, Chi-Cheng Lee, Guoqing Chang, BaoKai Wang, Nasser Alidoust, Guang Bian, Madhab Neupane, Chenglong Zhang, Shuang Jia, Arun Bansil, Hsin Lin, and M. Zahid Hasan arXiv:1501.00755 (unpublished).
- [24] H. M. Weng *et al.*, arXiv:1501.00060 (unpublished).
- [25] C. L. Zhang *et al.*, arXiv:1502.00251 (unpublished).



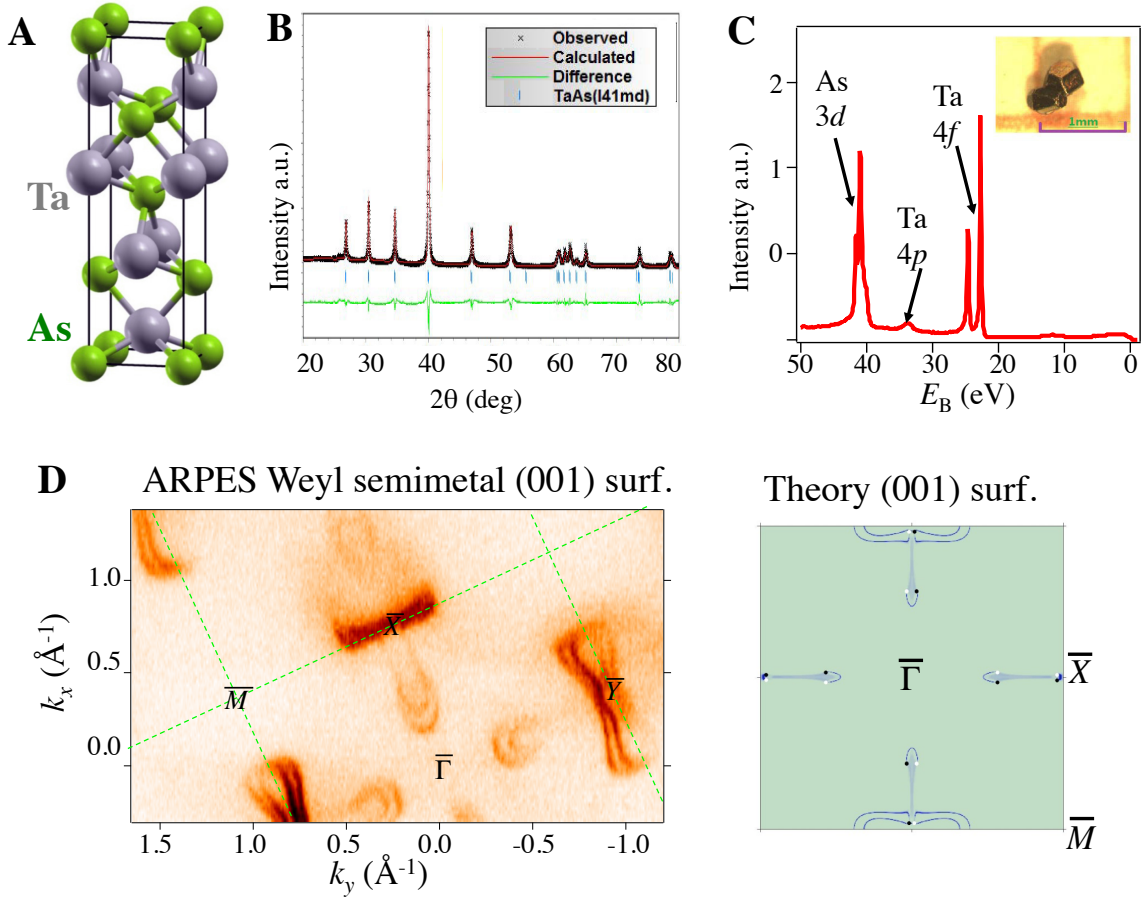


FIG. 1: **The crystal structure and an overview of the electronic structure of TaAs.** **a**, Boby-centred tetragonal structure of TaAs, shown as stacked TaAs layers. An electric polarization is induced due to dimples in the TaAs lattice. The arrangement of Ta atoms for each layer (Ta<sub>1</sub> to Ta<sub>4</sub>) is illustrated in the bottom-right panel. **b**, X-ray diffraction measurements showing the lattice parameters matching well with the space group of I4<sub>1</sub>md. **c**, ARPES core level spectrum showing clear Ta 4*f* and As 3*d* core level peaks. **d**, The Fermi surface of the (001) cleaving plane of TaAs, showing Fermi arcs near the  $\bar{X}$  point, near the  $\bar{Y}$  point, near the midpoint of the  $\bar{X}$  point and the  $\bar{\Gamma}$  point and near the midpoint of the  $\bar{Y}$  point and the  $\bar{\Gamma}$  point. **e**, An *ab initio* band structure calculation of the surface states on the (001) surface of TaAs, in agreement with our experimental data.

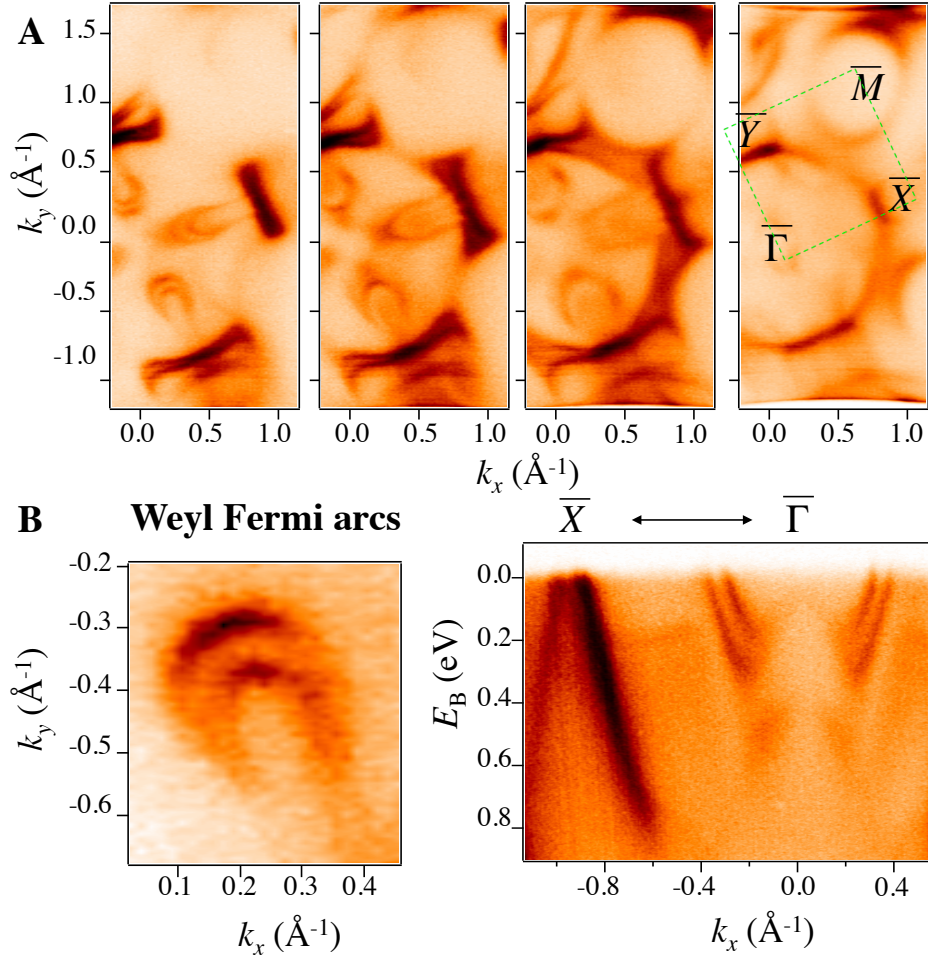


FIG. 2: **Fermi arc surface states on the (001) surface of TaAs.** **a**, ARPES spectra of the band structure of TaAs. The square Brillouin zone and  $C_4$  rotation symmetry deep in the bulk shows that the sample is cleaved on the (001) surface. The strong  $C_4$  violation by certain bands at shallow binding energies is consistent with  $C_4$  screw axis symmetry broken by the (001) surface and clearly shows that the  $C_4$  asymmetric states are surface states. These states consist of Fermi arcs and are observed near the  $\bar{X}$  point, near the  $\bar{Y}$  point, near the midpoint of the  $\bar{X}$  point and the  $\bar{\Gamma}$  point and near the midpoint of the  $\bar{Y}$  point and the  $\bar{\Gamma}$  point. **b**, High-resolution ARPES Fermi surface mapping of the Fermi arc surface states near the midpoint of the  $\bar{X}$  point and the  $\bar{\Gamma}$  point. We clearly observe two Fermi arcs. Since the arcs terminate at arbitrary points of the Brillouin zone, they terminate at Weyl points. Since there are two arcs, the chiral charge of the Weyl points is  $\pm 2$ . Both of the Fermi arcs are consistent with the definition of chiral Weyl Fermi arcs.

ARPES spectra of the band structure of TaAs. The square Brillouin zone and  $C_4$  rotation symmetry deep in the bulk shows that the sample is cleaved on the (001) surface. The strong  $C_4$  violation by certain bands at shallow binding energies is consistent with  $C_4$  screw axis symmetry broken by the (001) surface and clearly shows that the  $C_4$  asymmetric states are surface states. These states consist of Fermi arcs and are observed near the  $\bar{X}$  point, near the  $\bar{Y}$  point, near the midpoint of the  $\bar{X}$  point and the  $\bar{\Gamma}$  point and near the midpoint of the  $\bar{Y}$  point and the  $\bar{\Gamma}$  point. High-resolution ARPES Fermi surface mapping of the Fermi arc surface states near the midpoint of the  $\bar{X}$  point and the  $\bar{\Gamma}$  point. We clearly observe two Fermi arcs. Since the arcs terminate at arbitrary points of the Brillouin zone, they terminate at Weyl points. Since there are two arcs, the chiral charge of the Weyl points is  $\pm 2$ . Both of the Fermi arcs are consistent with the definition of chiral Weyl Fermi arcs.

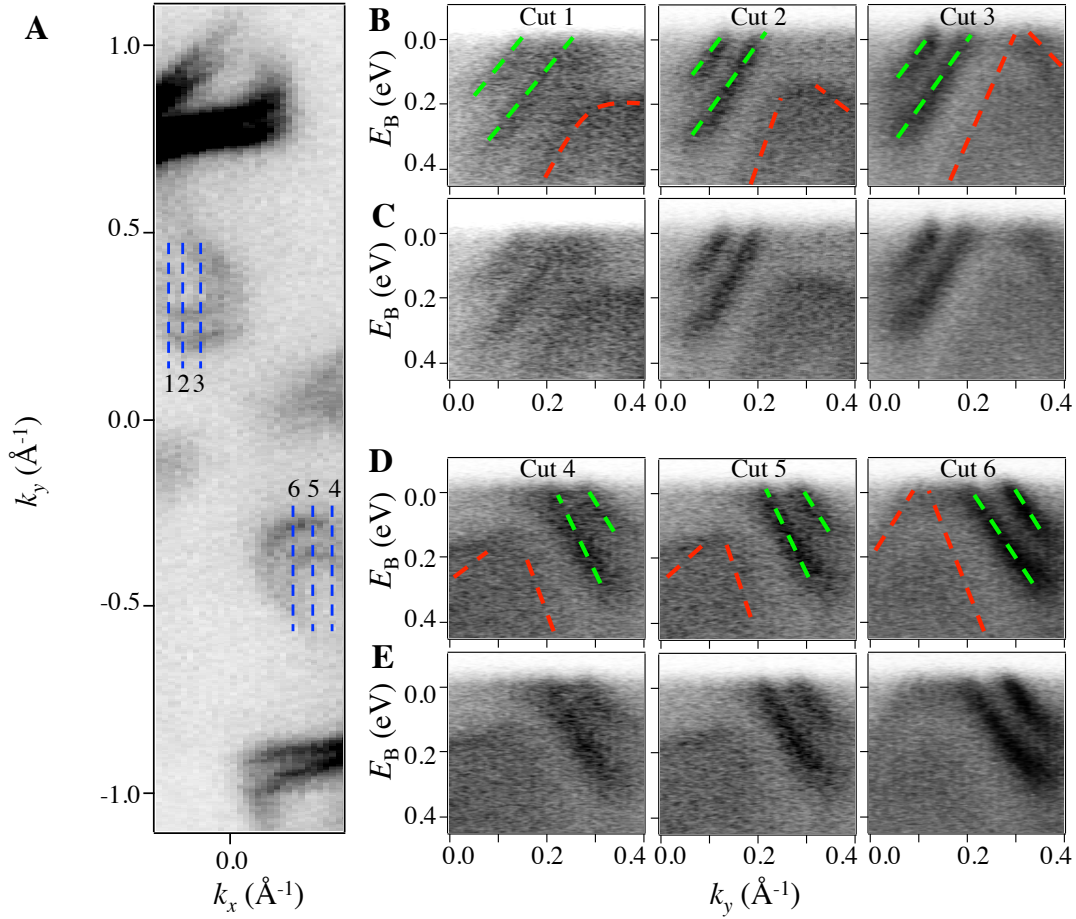


FIG. 3: **Fermi arc surface states in TaAs.**

FIG. 3: **Weyl cones in TaAs.** **a**, A Fermi surface map to show the direction of cuts presented in **b-e**. **b, c**, ARPES spectra taken along a succession of parallel cuts on an oblique direction in the Brillouin zone, as indicated by 1, 2, 3 in panel **a**. We observe a Weyl cone nested with the Fermi arc surface states which disperses as a function of in-plane momentum and rises up toward the Fermi level to meet the Fermi arcs. This Weyl cone is in agreement with *ab initio* bulk band structure calculations on the TaAs. **d, e**, ARPES spectra along 4, 5, 6 cuts in **a** showing another Weyl cone, which is a  $C_4$  rotated cousin of the first, also in agreement with *ab initio* bulk band structure calculations on the TaAs. Red and green dotted lines in **b** and **d** are guides-to-the-eye highlighting the bulk Weyl bands and surface states in **c** and **e**, respectively.

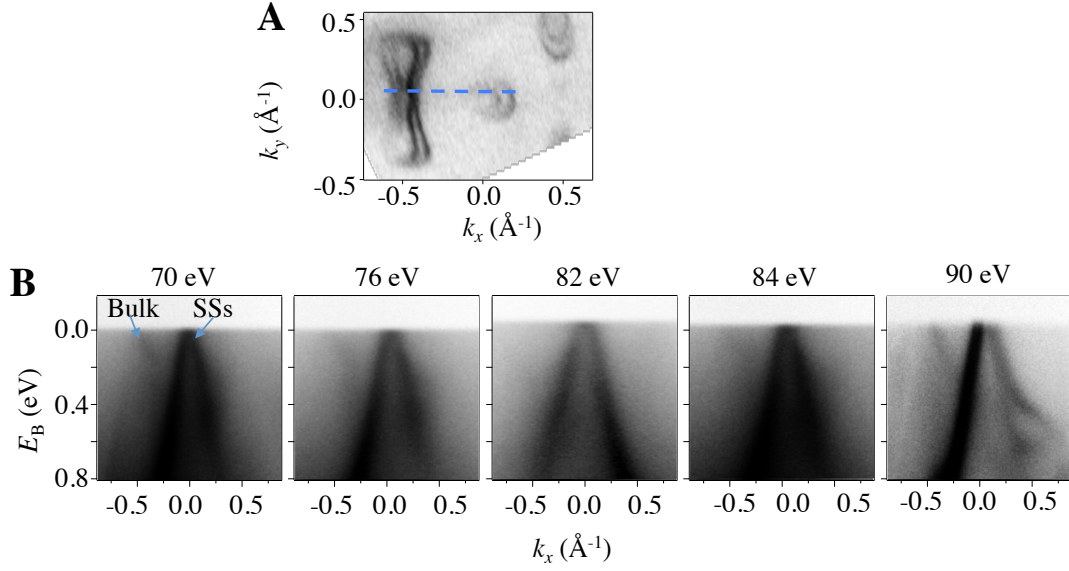


FIG. 4: **Dispersion in  $k_z$  in TaAs.** **a**, A Fermi surface map to show the direction of cut used for photon energy dependence measurements presented in **b**. **b**, ARPES spectra along the  $\bar{\Gamma}$ - $\bar{X}$  high-symmetry direction taken at a succession of incident photon energies  $h\nu$  to probe different  $k_z$ . We observe clear changes in the bulk bands as we vary  $h\nu$ , showing a three-dimensional band structure in TaAs. At the same time, the surface state bands are independent of incident photon energy, providing further evidence that we have observed Fermi arc surface states in TaAs.